THE GLOBAL OSCILLATION NETWORK GROUP SITE SURVEY

II. *Results*

FRANK HILL[1], GEORGE FISCHER[1,2], SUZANNE FORGACH[1], JENNIFER GRIER[1,3], JOHN W. LEIBACHER[1], HARRISON P. JONES[4], PATRICIA B. JONES[5], RENATE KUPKE[1,6], ROBIN T. STEBBINS[7], DONALD W. CLAY[8], ROBERT E. L. INGRAM[8], KENNETH G. LIBBRECHT[9], HAROLD ZIRIN[9], ROGER K. ULRICH[10], LAWRENCE WEBSTER[10], LESTER S. HIEDA[6], BARRY J. LABONTE[6], WAYNE M. T. LU[6], EDWIN M. SOUSA[6], CHARLES J. GARCIA[11], ERIC A. YASUKAWA[11], JOHN A. KENNEWELL[12], DAVID G. COLE[12], HUANG ZHEN[13], XIAO SU-MIN[13], ARVIND BHATNAGAR[14], ASHOK AMBASTHA[14], ABDULRAHMAN SA'AD AL-KHASHLAN[15], MUHAMMAD-SALEH ABDUL-SAMAD[15], ZOUHAIR BENKHALDOUN[16], SAMIR KADIRI[16], FRANCISCO SÁNCHEZ[17], PERE L. PALLÉ[17], OSCAR DUHALDE[18], HERNAN SOLIS[18], OSCAR SAÁ[19] and RICARDO GONZÁLEZ[19]

(Received 19 January, 1994; in revised form 17 March, 1994)

[1] National Solar Observatory, National Optical Astronomy Observatories, Tucson, AZ 85726, U.S.A. The National Optical Astronomy Observatories are operated by the Association of Universities for Research in Astronomy, Inc. (AURA) under cooperative agreement with the National Science Foundation.
[2] Mathematics Department, University of Utah, Salt Lake City, UT 84112, U.S.A.
[3] Lunar and Planetary Laboratory, University of Arizona, Tucson, AZ 85721, U.S.A.
[4] NASA/GSFC, Southwest Station, NOAO, Tucson, AZ 85726, U.S.A.
[5] Center for Computing and Information Technology, University of Arizona, Tucson, AZ 85721, U.S.A.
[6] Institute for Astronomy, University of Hawaii, Honolulu, HI 96822, U.S.A.
[7] Joint Institute for Laboratory Astrophysics, University of Colorado, Boulder, CO 80309, U.S.A.
[8] Arizona Western College, Yuma, AZ 85366, U.S.A.
[9] Big Bear Solar Observatory, California Institute of Technology, Pasadena, CA 91125, U.S.A.
[10] Mt. Wilson Observatory, University of California at Los Angeles, CA 90024, U.S.A.
[11] Mauna Loa Solar Observatory, High Altitude Observatory, Boulder, CO 80307, U.S.A.
[12] Learmonth Solar Observatory, IPS Radio and Space Services, West Chatswood, New South Wales, Australia.
[13] Urumqi Astronomical Station, Academia Sinica Xinjiang, Urumqi, China.
[14] Udaipur Solar Observatory, Physical Research Laboratory, Udaipur, India.
[15] King Abdul Aziz City for Science and Technology, Riyadh, Saudi Arabia.
[16] Centre National de Coordination et de Planification de la Recherche Scientifique et Technique, Rabat, Morocco.
[17] Observatorio del Teide, Instituto Astrofisica de Canarias, Tenerife, Spain.
[18] Las Campanas Observatory, The Observatories of the Carnegie Institution of Washington, Pasadena, CA 91101, U.S.A.
[19] Cerro Tololo Interamerican Observatory, National Optical Astronomy Observatories, Tucson, AZ 85726, U.S.A.

Solar Physics **152:** 351–379, 1994.

Abstract. The Global Oscillation Network Group (GONG) Project will place a network of instruments around the world to observe solar oscillations as continuously as possible for three years. The Project has now chosen the six network sites based on analysis of survey data from fifteen sites around the world. The chosen sites are: Big Bear Solar Observatory, California; Mauna Loa Solar Observatory, Hawaii; Learmonth Solar Observatory, Australia; Udaipur Solar Observatory, India; Observatorio del Teide, Tenerife; and Cerro Tololo Interamerican Observatory, Chile.

Total solar intensity at each site yields information on local cloud cover, extinction coefficient, and transparency fluctuations. In addition, the performance of 192 reasonable networks assembled from the individual site records is compared using a statistical principal components analysis. An accompanying paper describes the analysis methods in detail; here we present the results of both the network and individual site analyses.

The selected network has a duty cycle of 93.3%, in good agreement with numerical simulations. The power spectrum of the network observing window shows a first diurnal sidelobe height of 3×10^{-4} with respect to the central component, an improvement of a factor of 1300 over a single site. The background level of the network spectrum is lower by a factor of 50 compared to a single-site spectrum.

1. Introduction

The motivation for a network of observing sites intended to obtain helioseismic data is discussed by Aindow *et al.* (1988), Hill (1990), and Fossat (1991). The essential requirements are that time lost to weather and instrumental problems be minimized and that the remaining gaps in the data record be distributed as randomly as possible.

The Global Oscillation Network Group (GONG) Project selected the six network sites starting with a simple two-parameter cloud cover model to simulate the observational conditions at a site (Hill and Newkirk, 1985). The two parameters are ρ, the mean fraction of time that the daytime sky is clear, and τ, the mean temporal length of clear weather. Estimates of ρ are obtained from climatological maps of the average sunshine hours in January and July, while τ is chosen to be either 0.5 or 2.5 days, representing mountain-top orographic clouds or the passage of storm systems, respectively. The model predicts that a well-chosen network of six sites will achieve an overall filling factor of 93.5%. To test this prediction, and to gain experience operating a network of instruments at several locations, the GONG Project assembled a Site Survey Instrument (Fischer *et al.*, 1986), and placed copies at 15 sites around the world.

An intermediate status report of the survey was published in 1988 (Hill *et al.*). Details of the data collection and description of the analysis techniques used to reduce the data are presented in the companion paper by Hill *et al.* (1994, Paper I). Here in Paper II, the results of the GONG Site Survey are presented. The records of clear time fraction, average seasonal clear time variations, distribution of extinction coefficient, and transparency power spectra are presented for each survey site. The results of a principal component analysis comparing both the 15 individual sites and the 192 possible networks are discussed. Finally, we investigate the sensitivity of the performance of the selected network to assumptions about the length of time lost to instrumental failures.

2. Description of the Individual Sites

The sites in the survey are Tucson, Arizona; Yuma, Arizona; Big Bear, California; Mt. Wilson, California; Mauna Kea, Hawaii; Mauna Loa, Hawaii; Haleakala, Hawaii; Learmonth, Australia; Urumqi, China; Udaipur, India; Riyadh, Saudi Arabia; Oukaimeden, Morocco; Tenerife, Spain; Las Campanas, Chile; and Cerro Tololo, Chile. The local geographic and institutional conditions at the sites are described in this section. The sites are grouped into six longitude bands as described in Table II of Paper I, reflecting the natural arrangement of a network imposed by the distribution of land on the Earth.

2.1. Band 1: the southwest US

Four sites are located in this band. Tucson is a city at an elevation of about 800 m in the Sonoran desert in southern central Arizona. The instrument is situated on the roof of the office building of the National Optical Astronomy Observatories. The headquarters of the GONG Project, administered by the National Solar Observatory, is also located in this building. Yuma is a city at an elevation of about 50 m in the desert in southwestern Arizona. Here, the instrument was placed on the roof of the Science and Mathematics Building at Arizona Western College. At Big Bear, the site survey instrument is located to the north of the dome at Big Bear Solar Observatory. This observatory is situated at an elevation of 2067 m on an island in an artificial lake in the San Bernardino Mountains in southern California, and is administered by the California Institute of Technology. A report of the original survey that selected this site in 1967 has been published by Zirin and Mosher (1988). The fourth station in this band is Mt. Wilson Observation at an elevation of 1742 m in the San Gabriel Mountains near Pasadena, California. A GONG Site Survey instrument was placed at the top of the 150-foot tower for a short period of time to allow intercomparison of GONG Site Survey data with data recorded by an all-sky brightness monitor. Data from the all-sky monitor were subsequently used as a proxy in the GONG Site Survey. The 150-foot tower is currently administered by the University of California at Los Angeles.

2.2. Band 2: Hawaii

Three high-altitude sites are located in this longitude band. One monitor was placed on the roof of the 88-inch telescope building at Mauna Kea Observatory, administered by the Institute for Astronomy, University of Hawaii. This site is located at an elevation of 4215 m on the summit of Mauna Kea. A second instrument is at the Mauna Loa Solar Observatory (MSLO), administered by the High Altitude Observatory in Boulder, Colorado. MLSO is located at an elevation of 3353 m on National Oceanic and Atmospheric Administration property situated on a lava field on the northwest flank of Mauna Loa on Hawaii. The last instrument in this band was situated at Mees Solar Observatory (MSO), administered by the Institute for Astronomy, University of Hawaii. MSO is at an elevation of 3054 m

on Haleakala, Maui. An instrument of the Birmingham Solar Oscillation Network (BISON) (Aindow *et al.*, 1988) is also located at Haleakala.

2.3. Band 3: Australia

A single site is located in this band at Learmonth Solar Observatory. This Observatory is situated at an elevation of 10 m on the western shore of Exmouth Gulf on the North West Cape of Australia and is co-administered by the IPS Radio and Space Services, headquartered in Chatswood, New South Wales, and the U.S. Air Force. Learmonth is also the site of one of the stations of the Solar Electro-Optical Network (SEON). A description of the site has been published by Kennewell and Cornelius (1983).

2.4. Band 4: Asia

Three sites are located in this band. Urumqi is situated at an elevation of 1000 m in Xinjiang province in northwestern China. The instrument was first located at the Urumqi Astronomical Station, administered by the Academia Sinica Xinjiang. To minimize the effects of an urban center, it was subsequently moved to two other nearby sites: first Lianmxin, and then Yong Feng. Udaipur is situated at an elevation of 750 m in a semi-arid highland region of western India. The instrument is located at the Udaipur Solar Observatory. A brief description of the original site survey and instrumentation of USO has been published by Ambastha and Bhatnagar (1985). The results of the GONG Site Survey for Udaipur have been published by Ambastha *et al.* (1991). USO is administered by the Physical Research Laboratory, headquartered in Ahmedabad. The third site in this band is Riyadh, the capital city of Saudi Arabia at an elevation of about 600 m in the Saudi Arabian Desert. Here, the instrument was located on the roof of a building in the King Abdul Aziz City of Science and Technnology. The longitude of Riyadh is such that it was also included in the next longitude band when the possible networks were constructed.

2.5. Band 5: Africa

Two stations are located in this band. Oukaimeden is a solar observing station located at an altitude of 2700 m in the Atlas Mountains of Morocco. The site is administered by the Centre National de Coordination et de Planification de la Recherche Scientifique et Technique, headquartered in Rabat. An instrument of the International Research on the Interior of the Sun (IRIS) helioseismology network (Fossat, 1991) is located at Oukaimeden, and a description of the site has been published by Benkhaldoun *et al.* (1991). Cloud-cover measurements from a three-band photometer at the site have been presented by Benkhaldoum *et al.* (1993). The second site in this band is located at an altitude of 2398 m at the Observatorio de Teide, administered by the Instituto Astrofisica de Canarias of the Universidad de la Laguna in Tenerife, Spain. Instruments of both IRIS and BISON are located at Teide. A description of the site has been published by Pallé (1991), and an analysis of solar observing conditions has been published by Brandt and Wöhl (1982).

2.6. Band 6: Chile

Two stations are located in this band. One instrument was located at Las Campanas Observatory, administered by The Observatories of the Carnegie Institution of Washington, in Pasadena, California. Las Campanas is at an altitude of 2282 m, and is also the site of an instrument in the BISON. The second site is Cerro Tololo, a mountain with an elevation of 2215 m approximately 130 km south of Las Campanas. The instrument is located at Cerro Tololo Interamerican Observatory, a division of the National Optical Astronomy Observatories headquarted in Tucson, Arizona.

3. Results of the Individual Site Analysis

3.1. Clear time fraction and cloud cover

One of the most important criteria for choosing a good helioseismic observing site is the fraction of clear time, C_w. This quantity is the proportion of time that the instrument measured an intensity at the level of 90% of the value expected at the top of the Earth's atmosphere. C_w is calculated only during the daylight times that the instrument is known to be operational. See Paper I for more details.

Several summary quantities covering the entire time available for each site are defined for the cloud cover measurements. They are presented in Tables I–IV, and their definitions are discussed more fully in Paper I. Table I describes the temporal extent of each site data set. Table II presents the cloud cover fractions: C_a, the fraction of clear time for the entire period; D_a, the fraction of dark time for the entire period; B_a, the fraction of instrumental downtime for the entire period; C_w, the fraction of clear time after removal of instrumental downtime and D_w, the fraction of dark time after the removal of instrumental downtime. Table III displays counts of completely clear, dark, and lost days. Table IV summarizes long-term aspects of the cloud cover.

Figure 1 presents plots of the 30-day block average of C_w as a function of time for the individual sites. The plots for Yuma, Mauna Loa, Riyadh, and Las Campanas have intervals during which no measurements of C_w were obtained due to instrumental problems. These episodes are represented by breaks in the plotted measurements. The results presented for Big Bear and Oukaimeden ignore a portion of the data obtained at the beginning of the runs at these sites when circumstances prevented the collection of valid data. At Big Bear, a period of about 9 months is ignored due to the inference of trees at the original site of the instrument. At Oukaimeden, the first 2.5 months of data are neglected due to instrumental start-up difficulties. The analysis for Urumqi is performed on the combined data from all three Chinese sites. The values of C_w for Mt. Wilson are obtained from the strip chart records of the all-sky monitor, as discussed in Paper I. It is not always possible to determine whether the sky was clear or cloudy by visually inspecting these records, and so such periods are classified as 'broken' for that reason, even

TABLE I

Individual site data temporal extent

Site	Start date of data	End date of data	Total days in data set	Total possible sunshine hours
Tucson	17 June, 1986	10 Sep., 1993	2643	28383
Yuma	16 July, 1985	28 Feb., 1991	2054	21800
Big Bear	30 May, 1986	8 Sep., 1993	2659	28617
Mt. Wilson	15 Apr., 1985	24 Sep., 1990	1989	21523
Mauna Kea	10 Dec., 1985	19 Mar., 1991	1926	20448
Mauna Loa	25 May, 1989	16 Sep., 1993	1576	16896
Haleakala	7 Dec., 1985	18 Dec., 1991	2203	23473
Learmonth	2 Dec., 1985	22 Aug., 1993	2821	29924
Urumqi	19 Dec., 1987	28 Feb., 1992	1533	16277
Udaipur	8 Nov., 1986	30 June, 1993	2427	25849
Riyadh	12 Oct., 1988	26 Feb., 1991	868	9101
Oukaimeden	1 Jan., 1989	23 Apr., 1991	843	8931
Teide	24 Sep., 1985	30 July, 1993	2867	30576
Cerro Tololo	8 Mar., 1986	6 Sep., 1993	2740	28892
Las Campanas	7 Mar., 1986	20 Apr., 1991	1871	19863

TABLE II

Individual site cloud cover percentage

Site	C_a	D_a	B_a	C_w	D_w
Tucson	63.97	33.80	2.23	65.43	34.57
Yuma	59.45	19.94	20.61	74.89	25.11
Big Bear	65.59	27.32	6.99	70.63	29.37
Mt. Wilson	59.28	32.49	8.23	64.60	35.40
Mauna Kea	57.17	21.78	21.05	72.41	27.59
Mauna Loa	58.07	31.29	10.64	64.98	35.02
Haleakala	55.65	30.72	13.63	64.43	35.57
Learmonth	73.66	21.36	4.98	77.52	22.48
Urumqi	31.99	51.41	16.60	38.36	61.64
Udaipur	56.93	33.56	9.51	62.91	37.09
Riyadh	35.93	22.06	42.01	61.96	38.04
Oukaimeden	39.57	39.03	21.39	50.34	49.66
Teide	67.14	26.89	5.97	71.41	28.59
Cerro Tololo	72.26	21.77	5.97	76.85	23.15
Las Campanas	77.06	16.65	6.29	82.23	17.77

TABLE III
Individual site daily quantities

Site	Total days in data set	Number of completely clear days	Number of completely dark days	Number of completely lost days	Mean time between failures (days)
Tucson	2643	725	220	22	48.18
Yuma	2054	772	130	324	2.19
Big Bear	2659	950	200	128	8.22
Mt. Wilson	1989	760	376	119	5.80
Mauna Kea	1926	691	145	314	2.10
Mauna Loa	1576	470	120	127	4.95
Haleakala	2203	581	233	245	3.35
Learmonth	2821	1359	173	86	13.16
Urumqi	1533	91	442	158	3.51
Udaipur	2427	740	319	67	13.73
Riyadh	868	163	70	281	0.78
Oukaimeden	843	134	124	129	2.23
Teide	2867	1213	257	111	10.51
Cerro Tololo	2740	1368	264	64	17.15
Las Campanas	1871	1133	128	85	9.02

though the instrument may have been actually operating. This may artificially inflate the failure statistics for Mt.Wilson.

The time histories of C_w in Figure 1 show annual variations strongly at some sites (e.g., Cerro Tololo, Udaipur), and not so strongly at others (e.g., Haleakala, Oukaimeden). Tucson shows a bi-annual cycle. The seasonal variations are accentuated in Figure 2, which presents C_w averaged into twelve calendar monthly bins. Figure 2 clearly shows seasonal variations such as the Boreal summer monsoons at Udaipur, the two rainy seasons in Tucson, the clear Boreal summer at Mt. Wilson, and the remarkably clear Austral summers at Cerro Tololo, Las Campanas, and Learmonth.

3.2. EXTINCTION COEFFICIENTS

The GONG Site Survey also provides measurements of the extinction coefficient, κ, at the sites. Figure 3 presents the observed statistical distribution of κ for the individual sites. The effects of altitude are clearly evident in this figure: the high-altitude sites (e.g., Mauna Kea) have a narrowly peaked distribution centered at low values of κ, while low-altitude sites such as Tucson have a broader distribution. Table V summarizes some statistical measures of the extinction coefficient.

TABLE IV
Individual site long-term quantities

Site	Longest string of completely clear days	Start of longest string of completely clear days	Longest string of completely dark days	Start of longest string of completely dark days	Longest string of completely lost days	Start of longest string of completely lost days
Tucson	10	30 Nov., 1989	7	2 July, 1986	3	1 Sep., 1990
Yuma	11	18 Aug., 1989	13	16 May, 1990	36	19 Aug., 198(
Big Bear	11	2 Nov., 1989	13	1 Jan., 1993	27	28 June, 1992
Mt. Wilson	21	27 June, 1988	11	7 Mar., 1986	17	23 Oct., 1987
Mauna Kea	14	25 Dec., 1985	9	15 Jan., 1990	27	13 Feb., 1991
Mauna Loa	13	17 Jan., 1992	8	23 Aug., 1991	41	7 July, 1992
Haleakala	16	3 Jan., 1986	7	27 Feb., 1990	23	12 Jan., 1991
Learmonth	24	29 Aug., 1990	5	5 June, 1990	13	22 Apr., 1986
Urumqi	2	17 June, 1988	13	12 Nov., 1988	17	18 Apr., 1991
Udaipur	13	19 Oct., 1987	14	30 July, 1988	10	6 Feb., 1988
Riyadh	9	17 Dec., 1989	6	30 Mar., 1989	153	30 May, 1990
Oukaimeden	9	11 Nov., 1990	6	19 Dec., 1989	25	15 July, 1989
Teide	17	9 June, 1989	7	18 Mar., 1990	29	27 Jan., 1989
Cerro Tololo	28	25 Dec., 1989	8	8 July, 1987	9	30 Sep., 1988
Las Campanas	32	1 Jan., 1988	9	8 July, 1987	61	8 Feb., 1990

3.3. TRANSPARENCY POWER SPECTRA

Power spectra of the transparency fluctuations at the sites are computed from the central seven hours of all days were completely clear at each site. Figure 4 shows the global average transparency power spectrum for the 9718 days currently available in the data base, along with the average power in the g-mode and p-mode bands defined in Paper I. The spectrum is well-described by a straight line in a log-log plot. A least-squares fit of the average spectrum resumts in an estimated functional form of

$$\log P(\nu) = -9.50 - 1.49 \log \nu \, .$$

Figure 5 displays the average spectra for all 15 individual sites. It can be seen that the slope of the spectrum is independent of site except for the high-frequency region ($\nu > 3$ mHz) of the spectra obtained at Learmonth, Teide, and Urumqi. Table VI provides the number of spectra, g-mode band power, p-mode band power, and fitted values of intercept and slope of the individual site transparency spectra.

TABLE V

Individual site extinction coefficients statistics

Site	Average	Standard deviation	Percent >0.1	Percent >0.2	Percent >0.3	Number of measurements
Tucson	0.1643	0.0414	96.93	25.03	0.00	673270
Yuma	0.1539	0.0377	96.01	14.84	0.00	780919
Big Bear	0.1206	0.0456	66.41	8.25	0.00	728635
Mt. Wilson	0.1270	0.0359	83.28	4.81	0.00	99238
Mauna Kea	0.0743	0.0147	5.43	0.00	0.00	789515
Mauna Loa	0.0930	0.0263	41.89	0.00	0.00	331501
Haleakala	0.0943	0.0158	45.13	0.00	0.00	798492
Learmonth	0.1724	0.0382	98.78	29.85	0.00	808324
Urumqi	0.1914	0.0718	92.51	44.72	10.49	219043
Udaipur	0.2071	0.0544	98.39	58.33	1.99	285969
Riyadh	0.2239	0.0660	99.28	64.54	17.93	129816
Oukaimeden	0.1215	0.0464	67.35	9.53	0.00	219502
Teide	0.1169	0.0397	62.29	2.16	0.00	688625
Cerro Tololo	0.1202	0.0349	73.87	1.62	0.00	779938
Las Campanas	0.1113	0.0234	77.31	0.26	0.00	965332

TABLE VI

Individual site transparency power-spectrum parameters

Site	Number of spectra	g-mode band power $\times 10^4$	p-mode band power $\times 10^6$	Fitted intercept	Fitted slope
Tucson	795	2.46	1.42	−10.30	−1.73
Yuma	696	3.25	2.11	−9.99	−1.68
Big Bear	1016	4.44	1.90	−9.93	−1.65
Mt. Wilson	61	7.05	3.61	−9.37	−1.52
Mauna Kea	551	1.30	0.96	−9.84	−1.50
Mauna Loa	384	2.49	1.40	−9.74	−1.52
Haleakala	590	0.92	1.16	−9.33	−1.34
Learmonth	1296	1.87	1.93	−8.66	−1.18
Urumqi	104	7.70	6.48	−8.23	−1.23
Udaipur	516	10.44	4.36	−10.09	−1.83
Riyadh	128	8.28	5.58	−9.74	−1.73
Oukaimeden	110	3.08	1.90	−9.88	−1.62
Teide	1106	2.21	2.64	−8.59	−1.19
Cerro Tololo	1338	1.29	1.39	−10.00	−1.58
Las Campanas	1027	1.24	1.22	−9.86	−1.51

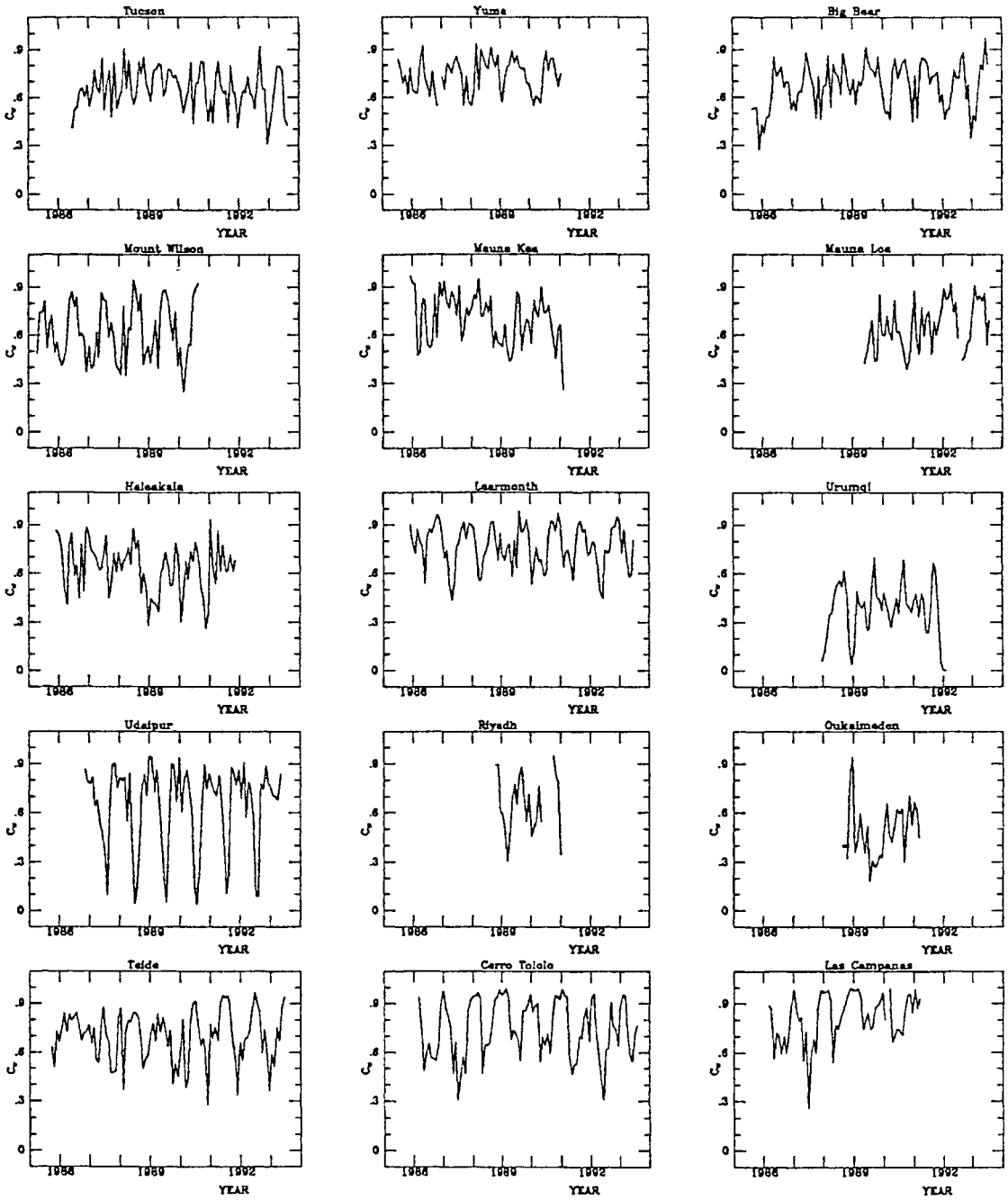

Fig. 1. The 30-day moving average of measured clear time fraction, C_w, for the 15 individual sites.

3.4. Comparison of the Sites Using Principal Components Analysis

The individual sites are compared and ranked using Principal Components Analysis (PCA) as described in Paper I. Briefly, the matrix of cross-correlations among the six variables is decomposed into its eigenvalues and eigenvectors. These are then used to provide an orthogonal (in the sense of being uncorrelated) set of variables called principal components (PCs) which are linear combinations of the original variables. Because a correlation matrix is used as input for the PCA, the weightings of the variables on the PCs are scale-independent. The eigenvalue for each PC is

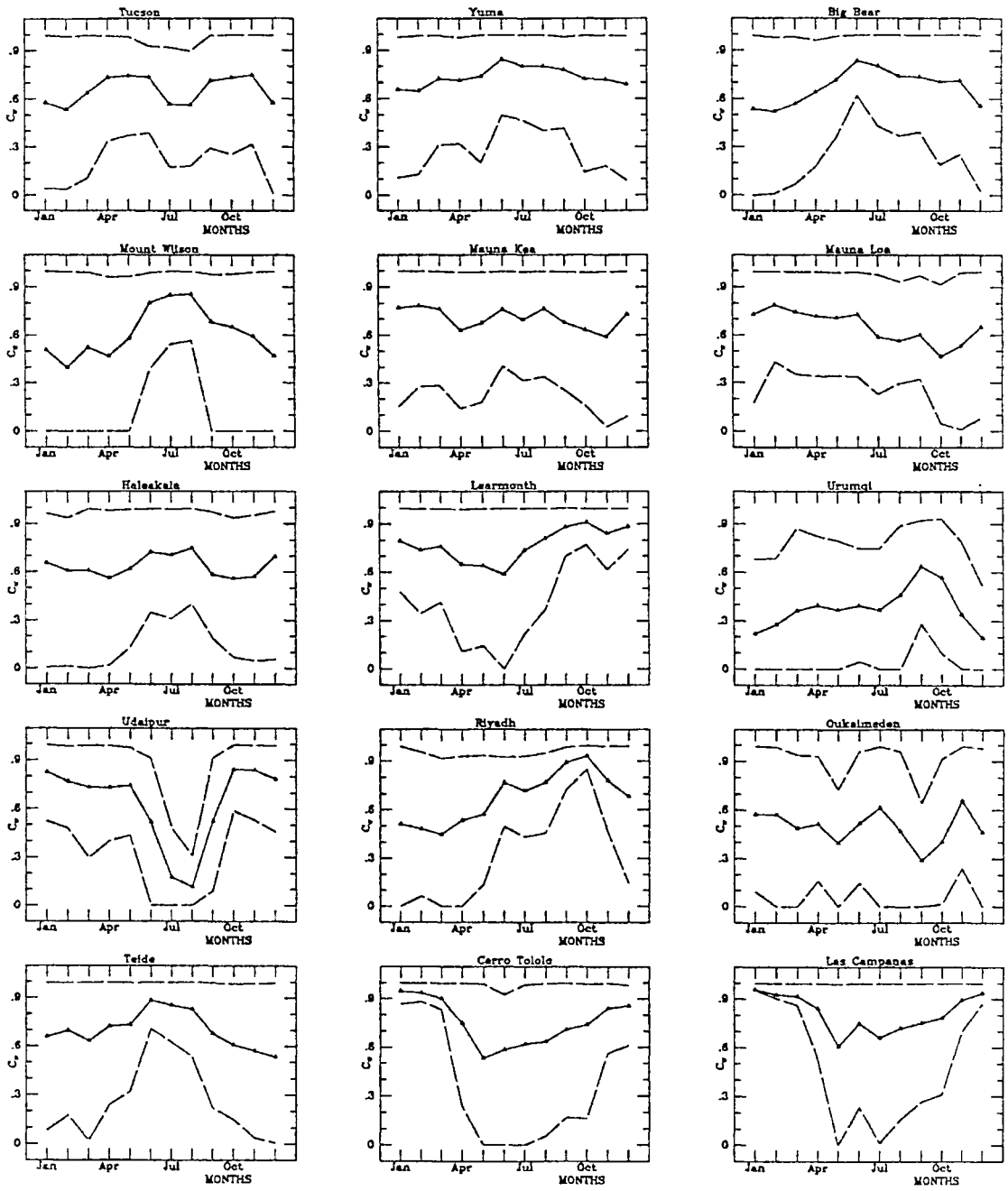

Fig. 2. The calendar month average of clear time fraction, C_w, for the individual sites. The triangles connected by a solid line represent the average value. The two dashed lines show the 15th and 85th percentile values.

then examined to determine its importance relative to the other PCs, and a subset of PCs is selected to yield a more parsimonious basis for the data set. The standardized score on each selected PC (corrected for the mean and divided by the standard deviation of the PC) is used to rank the sites.

For each site, Table VII summarizes the measurements of the six parameters used in the PCA. Note that some of the measured parameters in this table are different from those in Tables I–VI; this is due to the different time periods considered in

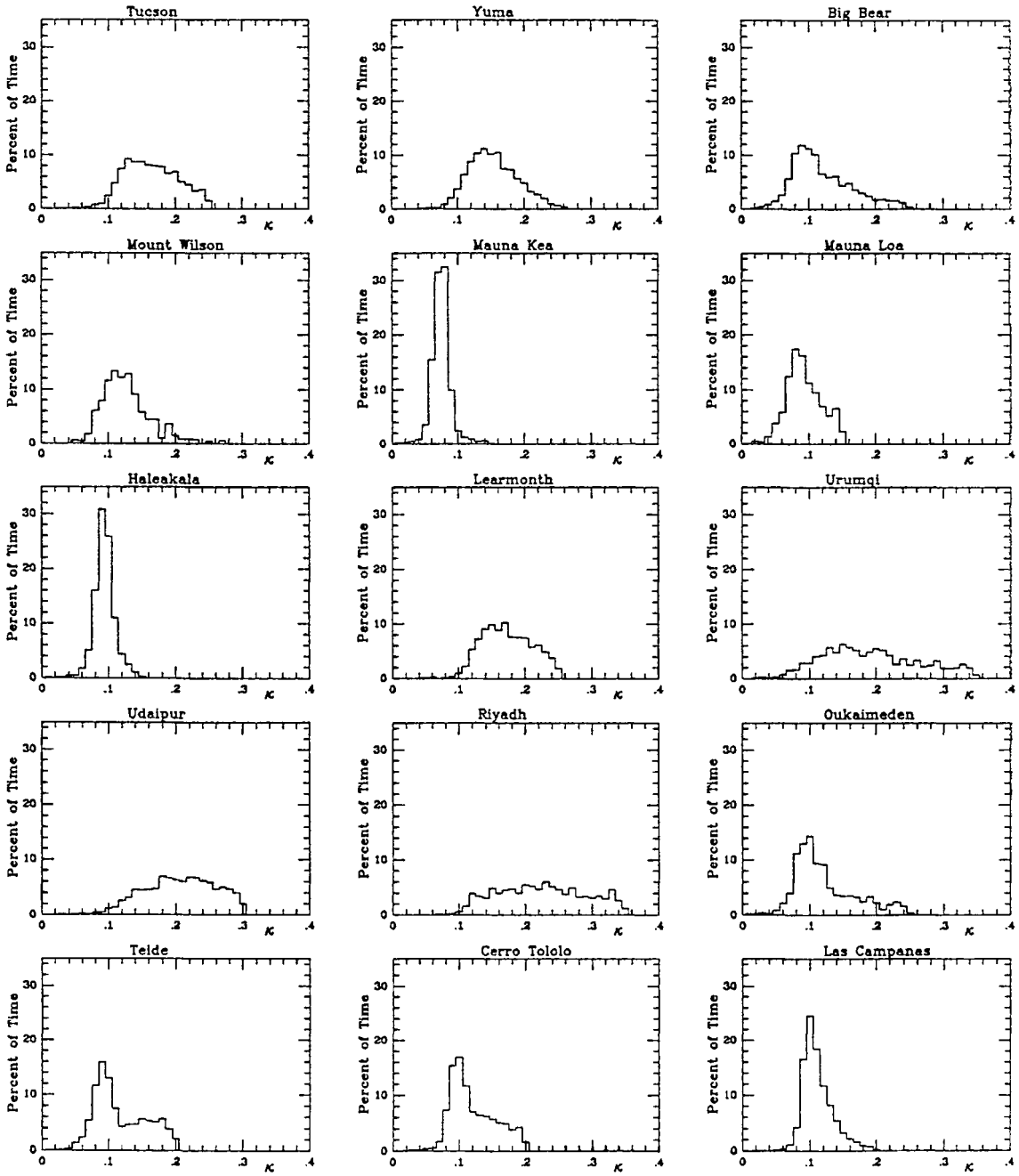

Fig. 3. The statistical distribution of the extinction coefficient, κ, at the individual sites.

the PCA (data up to early 1991), and in the tables (data up to September 1993). In addition, a different normalization is used in computing the transparency power spectra. Since the normalization is a constant multiplicative factor for all sites, the results of the PCA are independent of the normalization of the transparency parameters. Table VIII shows the correlation matrix for the individual sites. The sense of variables is such that high scores for clear weather percentage (CWPCT) and the intangibles (NTNG) and low scores for the other variables characterize desirable sites. The signs of the correlation coefficients conform to this pattern.

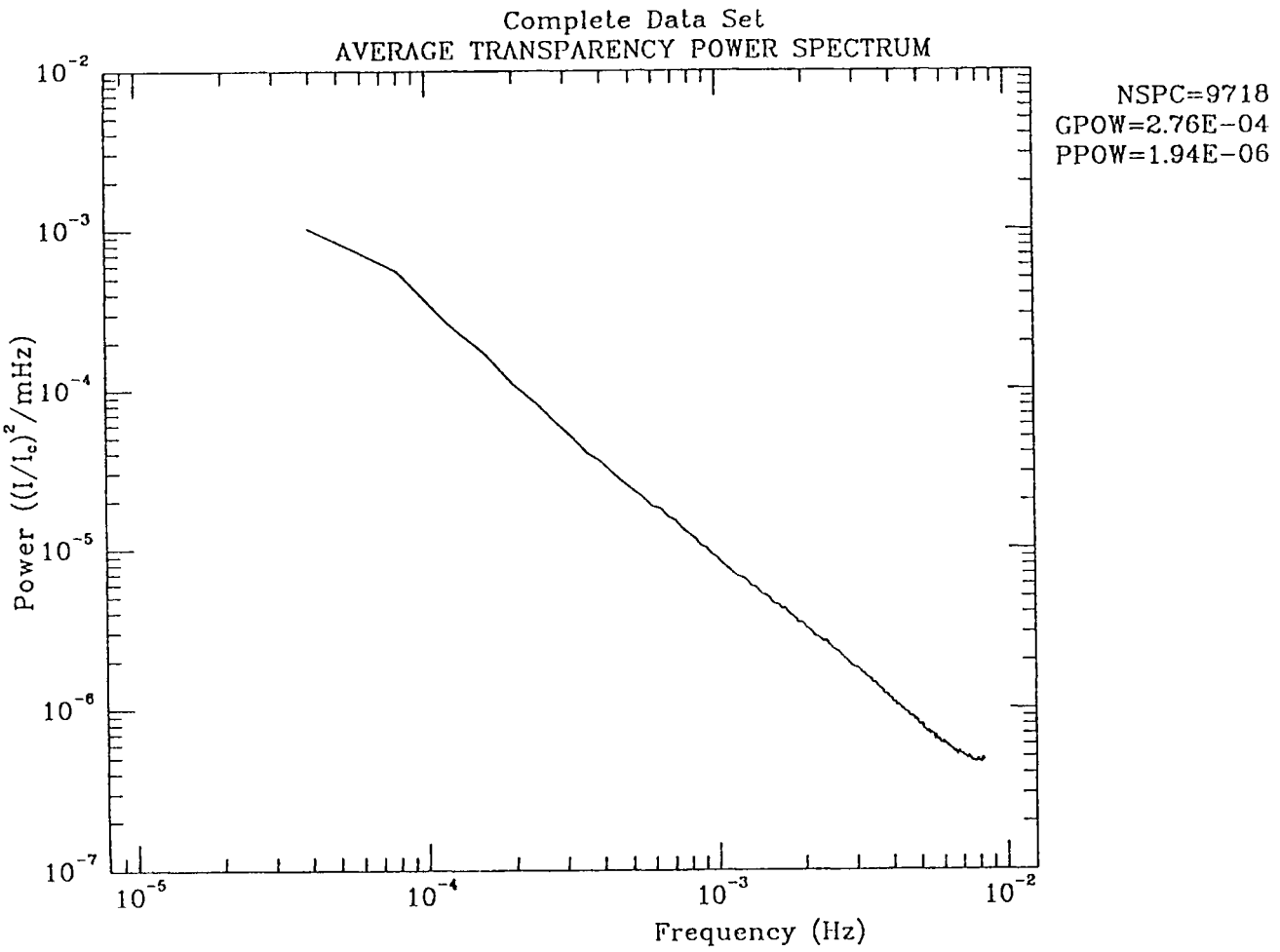

Fig. 4. The global average transparency fluctuations power spectrum obtained from the central seven hours of completely clear days at all of the individual sites. The quantities on the side are the number of spectra in the average (NSPC), the average power in a g-mode band with frequency $80\,\mu\text{Hz} \leq \nu \leq 200\,\mu\text{Hz}$ (GPOW), and the average power in a p-mode band with frequency $2000\,\mu\text{Hz} \leq \nu \leq 4000\,\mu\text{Hz}$ (PPOW). The average power spectrum is described by the functional form $\log P(\nu) = -9.50 - 1.49 \log \nu$.

Tables IX and X show the eigenvalues and projection pattern for the two dominant PCs for the individual site data. Since the magnitude of the eigenvalues depends, in part, on the number of variables in the analysis, it is easier to determine which PCs to select based on the percentage of the trace of the matrix analyzed which is attributable to each eigenvalue. Table IX also shows these percentages for the individual site data. The projection pattern is formed by the correlation coefficients between the eigenvector and the specified variable which are directly proportional to the weights of the linear combinations used to form the eigenvector and standardized PCs scores. Thus, coefficients whose absolute value is less than

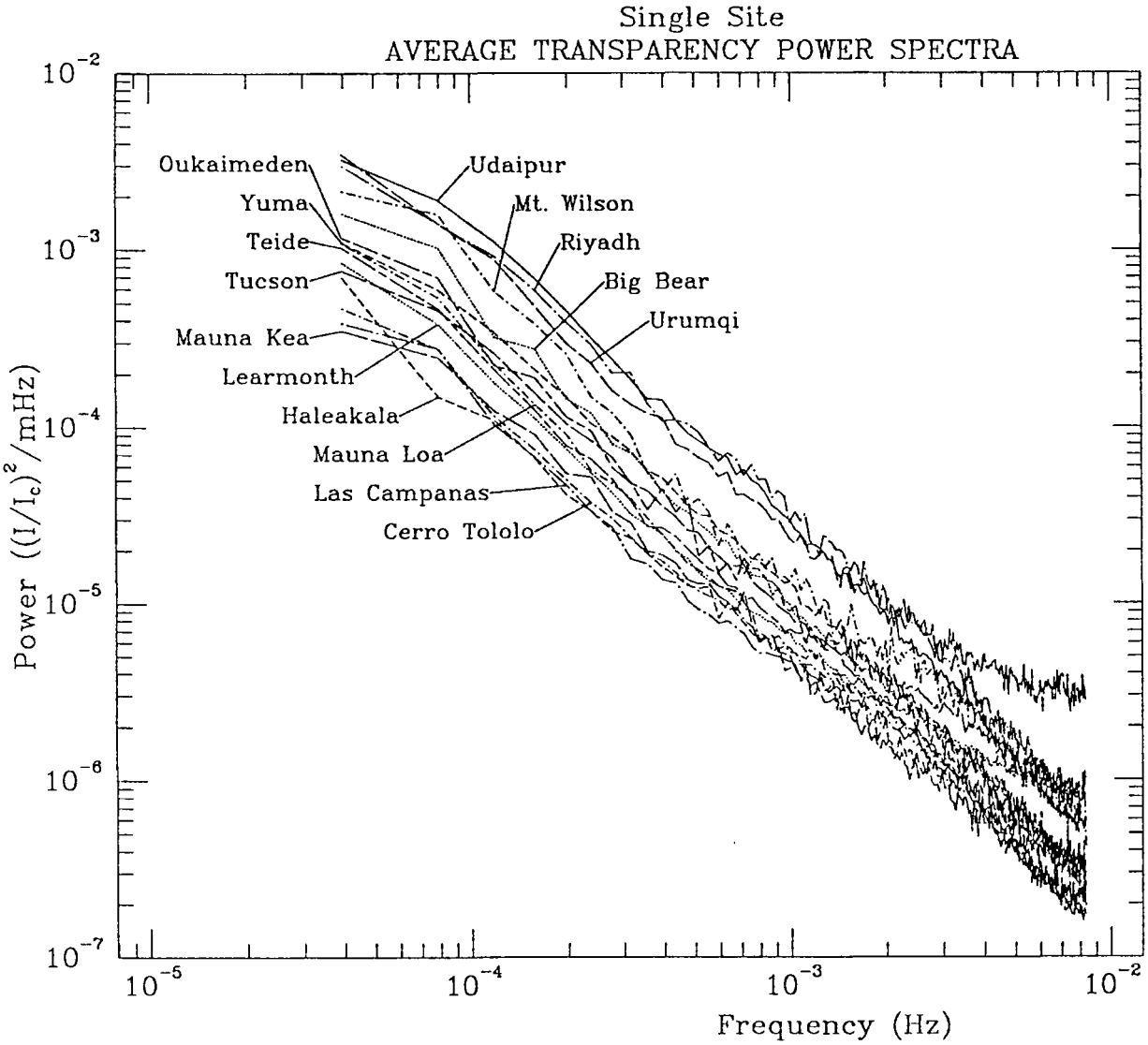

Fig. 5. The average power spectra for the individual sites. The parameters of the spectra are given in Table VI.

0.5 show marginal relationship between PC and variable. The PCs of a normalized eigenvector are determinate only to within a phase so that the sense of a given PC score relative to the desirability of the site must be determined by inspection. The dominant PC ($c1$ in Table X) correlated highly with quantities that one would physically expect to be good figures of merit for site performance for helioseimology. It accounts for nearly two-thirds of the standardized total variance of the sample; except for somewhat weaker correlation with broken percentage; it shows approximately uniform weighting across the original variables and has the sense that a low score is desirable. The second PC ($c2$ in Table X) accounts for only about one-sixth of the total standard variance and is not highly correlated with any of the original variables except for broken percentage. Indeed, whatever its importance in statistical representation of the sample, the second PC does not form a sensible helioseismic figure of merit. For example, depending on the overall sense assigned

TABLE VII

Individual site parameters used in PCA

Site	CWPCT clear weather percentage	BCPT instrument down time percentage	EXTN mean extinction	GPOW$\times 10^4$ g-mode transparency power	PPOW$\times 10^6$ p-mode transparency power	NTNG intangible score
Tucson	67.53	1.93	0.1493	1.95	1.10	5.00
Yuma	75.15	18.55	0.1546	2.60	1.68	3.62
Big Bear	71.41	4.47	0.1172	3.34	1.42	4.00
Mt. Wilson	65.15	8.22	0.1270	5.60	2.87	3.25
Mauna Kea	72.88	27.12	0.0745	1.04	0.77	3.38
Mauna Loa	58.10	4.67	0.0840	1.99	1.24	3.77
Haleakala	64.73	10.95	0.0941	0.53	0.88	3.64
Learmonth	78.10	4.53	0.1586	1.53	1.83	3.90
Urumqi	40.47	16.66	0.1870	5.68	5.51	1.70
Udaipur	60.94	9.26	0.2070	7.78	3.39	2.75
Riyadh	63.45	29.24	0.2252	6.46	4.41	1.18
Oukaimeden	47.27	24.70	0.1287	2.88	1.91	1.89
Teide	70.59	6.98	0.1025	1.91	2.33	4.00
Cerro Tololo	77.70	5.23	0.1072	0.96	1.05	4.25
Las Campanas	81.13	5.67	0.1101	0.96	0.93	3.91

TABLE VIII

Correlation matrix for individual sites

	CWPCT	BPCT	EXTN	GPOW	PPOW	NTGN
CWPCT	1.00	−0.35	−0.31	−0.51	−0.62	0.68
BPCT		1.00	0.26	0.26	0.35	−0.76
EXTN			1.00	0.79	0.78	−0.58
GPOW				1.00	0.84	−0.67
PPOW					1.00	−0.77
NTNG						1.00

to the PC, ranking by the second PC would select sites with low extinction and high broken percentage (or *vice versa*). We suspect that the projection patterns for all except the dominant PC would be unstable with sampling over different time periods and therefore use only the first PC to rank the sites.

Table XI shows the individual sites and standardized primary PC scores on the basis of $c1$ in Table I ranked in order from best to worst. Notice that the two South

TABLE IX

Eigenvalues of the correlation matrix for individual site data

Component	Eigenvalue	Percentage
1	3.92	65.4
2	1.05	17.4
3	0.65	10.8
4	0.18	2.9
5	0.14	2.4
6	0.07	1.1

TABLE X

Projection pattern for individual site data

	$c1$	$c2$
CWPCT	−0.72	0.21
BPCT	0.59	−0.72
EXTN	0.79	0.43
GPOW	0.87	0.37
PPOW	0.92	0.23
NTNG	−0.92	0.33

American sites rank highest with virtually identical scores and that the next seven sites are also very closely grouped. None of the best-ranked sites are more than a standard deviation above the mean. The site rankings are rearranged according to longitude band in Table XII. The standardized scores suggest that, on an individual site basis, Teide was the clear choice in band 5; Udaipur was the probable choice for band 4 where, however, all the sites are below average (a consequence of world weather patterns with respect to land mass); and that compelling evidence was lacking for selecting sites in bands 1, 2, and 6. Note that three of the six parameters (the average extinction coefficient, the g-mode band power, and the p-mode band power) are obtained over much shorter time periods for Mt. Wilson than for the other sites. Thus these results for Mt. Wilson are less reliable.

4. Results of the Network Analysis

As discussed in Paper I, a total of 192 reasonably distributed six-site networks can be constructed from the 15 candidate sites. In the interests of brevity, we do not

TABLE XI
Ordered primary component scores

Site	*id*	*z*
Cerro Tololo	ct	−0.99
Las Campanas	lc	−0.97
Tucson	tc	−0.76
Haleakala	ha	−0.68
Mauna Loa	ml	−0.55
Mauna Kea	mk	−0.55
Learmonth	lm	−0.52
Big Bear	bb	−0.51
Teide	iz	−0.51
Yuma	yu	−0.11
Mount Wilson	mw	0.33
Oukaimeden	ou	0.77
Udaipur	ud	1.18
Urumqi	ch	1.93
Riyadh	ry	1.95

TABLE XII
Site rankings by longitude bands

1		2		3		4		5		6	
tc	−0.76	ha	−0.68	lm	−0.52	ud	1.18	iz	−0.51	ct	−0.99
bb	−0.51	ml	−0.55			ch	1.93	ou	0.77	lc	−0.97
yu	−0.11	mk	−0.55			ry	1.94	ry	1.94		
mw	0.32										

present the detailed results for all 192 networks. Instead, we discuss the results of the PCA rankings of the networks. Examples of the analysis methods for the networks are presented in Paper I.

4.1. Principal Components Analysis of Network Performance

PCA is applied to the networks with the longitude partitioning of Table XII. Two slightly different time bases are used. The shorter time base covers a 384-day period when all the survey instruments were operating. The longer period includes the shorter with the addition of a few weeks when the Riyadh station was not operating but in principle could have been. Thirteen parameters are used to describe each network. A sample of these is displayed in Table III of Paper I. The dominant

TABLE XIII

Eigenvalues and projection patterns for 192 networks

	Short networks			Long networks		
	$c1$	$c2$	$c3$	$c1$	$c2$	$c3$
Eigenvalue	7.54	2.03	1.16	7.70	1.67	1.48
CMX	0.44	0.63	−0.30	0.13	0.05	0.81
DMX	−0.67	−0.10	−0.39	−0.35	−0.67	−0.24
CPCT	0.97	0.02	0.02	0.98	0.08	0.05
DPCT	0.01	−0.92	0.01	−0.55	0.68	0.09
BPCT	−0.92	0.31	−0.02	−0.88	−0.37	−0.10
NCD	0.90	0.32	−0.15	0.94	−0.01	0.16
SNRB	0.98	−0.04	0.06	0.97	0.14	0.04
SNFSL	0.93	−0.15	0.05	0.94	0.00	−0.17
HTFSL	−0.74	−0.12	0.10	−0.79	0.21	0.34
SNASL	0.94	−0.15	−0.08	0.95	−0.05	−0.12
AVOPD	−0.26	0.69	0.55	−0.72	0.47	0.03
ACI	0.75	0.17	−0.36	0.72	−0.17	0.50
ASW	0.64	−0.13	0.66	0.48	0.56	−0.55

eigenvalues and projection patterns for both time bases are displayed in Table XIII. For both samples the dominant PC accounts for nearly 60% of the total standardized variance while no other single PC accounts for more than about 15%. Notice that the projection patterns of the dominant PCs in both samples are consistent with a helioseismic figure of merit (better sites with higher scores), show high correlations with the clear percentage and spectral indices, and are very similar with each other. The subsidiary PCs correlate weakly with most of the original variables and the projection patterns vary markedly between the two samples. Again, we use only the dominant PC to rank the networks.

We are not in fact interested in the detailed rankings for all 192 possibilities, but only in the best combinations. Figure 6 shows the histogram of standardized PC scores for the long time base network evaluation. The histogram is similar for the shorter time period. In both rankings, three of the sites – Riyahd, Oukaimeden, and Urumqi – do not appear in networks with standard scores greater than 1.6. This is entirely consistent with the individual site rankings, so these sites are dropped from further consideration on the basis of this analysis.

Further PCA is applied to the 'best' networks. Of the remaining sites, Mauna Loa is dropped from the analysis (but not from further consideration) because of the late installation of its survey instrumentation and consequent short time base. The remaining sites can be configured into sixteen sensible networks (each of which contains Learmonth, Udaipur, and Teide) and are evaluted over a much longer time base of nearly four years. Since the use of 13 variables on a sample of 16

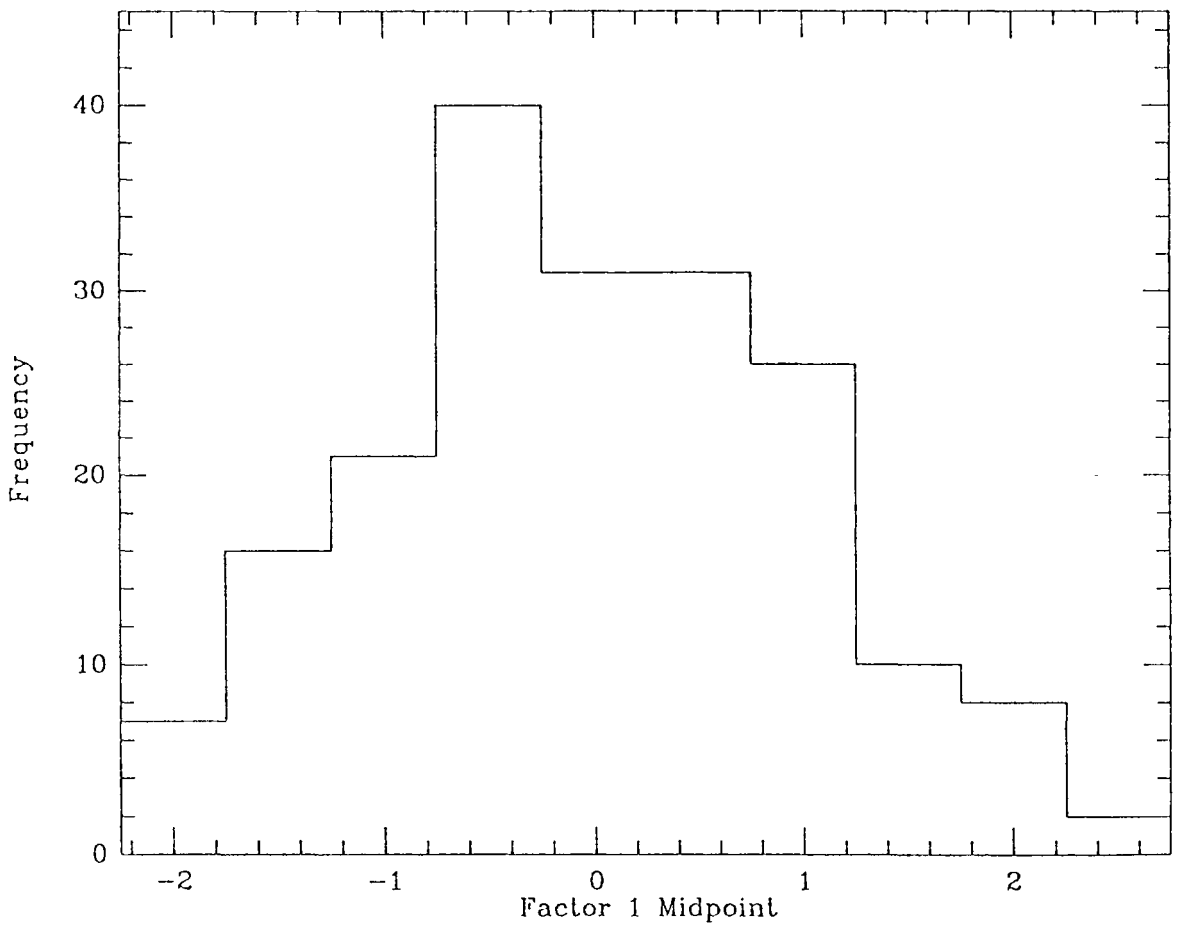

Fig. 6. Histogram of standard Principal Components Analysis scores of the long time base network evaluation.

does not leave sufficient statistical degrees of freedom for reliable interpretation of the results, we note that several of the original varibles are nearly constant for the 'good' networks (e.g., the mean clear-time fraction is 93.6% with a standard deviation of 0.13%) and select two subsets of variables that shows substantial variation over the sample. These subsets also appear to be fairly direct measures of quality for helioseismology. Both sets include the four power spectrum variables. The projection patterns of the dominant PCs for each variable subset are shown in Table XIV while Table XV shows the ordered listings of the standardized scores. The eigenvalues show the same previous pattern, albeit slightly less clearly, with the dominant PCs accounting for the rest in smaller individual proportions. For the top-ranked networks, the primary difference is to interchange Haleakala and Mauna Kea. Notice that the top-ranked network for the first choice of variables agrees with the network of top-ranked sites. Again, the statistical differences between the top several networks do not provide compelling evidence for making the remaining

TABLE XIV

Projection patterns for 16 good networks

	Set 1			Set 2	
	$c1$	$c2$		$c1$	$c2$
DPCT	0.52	−0.82	CLMAX	−0.64	0.52
BPCT	−0.82	0.49	DKMAX	−0.49	−0.21
SNRB	0.65	0.74	SNRB	0.81	0.48
SNFSL	0.94	0.28	SNFSL	0.98	0.00
HTFSL	0.60	−0.40	HTFSL	0.51	−0.67
SNASL	0.92	0.35	SNASL	0.95	0.20

TABLE XV

Ranked networks

Set 1				Set 2			
Network			Standard score	Network			Standard score
ha	tc	ct	1.68	mk	tc	ct	1.57
mk	tc	ct	1.51	ha	tc	ct	1.33
ha	bb	ct	0.89	mk	bb	ct	0.94
mk	bb	ct	0.73	ha	bb	ct	0.70
ha	tc	lc	0.70	mk	yu	ct	0.61
mk	tc	lc	0.48	mk	tc	lc	0.41
ha	mw	ct	0.20	ha	tc	lc	0.26
mk	bb	lc	−0.07	mk	bb	lc	0.04
ha	yu	ct	−0.07	ha	yu	ct	0.00
ha	bb	lc	−0.17	mk	mw	ct	−0.02
mk	yu	ct	−0.19	ha	mw	ct	−0.07
mk	mw	ct	−0.29	ha	bb	lc	−0.39
ha	yu	lc	−0.95	mk	yu	lc	−0.56
mk	yu	lc	−1.17	ha	yu	lc	−0.97
ha	mw	lc	−1.51	mk	mw	lc	−1.83
mk	mw	lc	−1.77	ha	mw	lc	−2.01

choices, but suggest that the choice in band 1 be restricted to Tucson and Big Bear.

A Site Selection Committee resolved the remaining choices on other grounds. In the case of the two South American sites (band 6) where both are excellent and virtually identical in performance, the Committee recommended Cerro Tololo on the grounds that the GONG Project is managed by NSO, a part of the same institutional structure as Cerro Tololo. In the case of band 3 (Hawaii), the committee recommended Haleakala on the basis of its high (often superior) ranking

and because it is the site of a well-established solar observatory operated by an institution with substantial expertise and interest in helioseismology. Mauna Kea is devoted to other disciplines and is a harsher environment in which to run and maintain a remote station. Mauna Loa was retained as a backup site because, at least for its limited time base, it ranks very closely with Haleakala. Indeed, the GONG Project eventually selected Mauna Loa as the Hawaiian site for logistical reasons. In the case of the Southwest United States sites, the committee was not able to make a clear choice between Tucson and Big Bear. Tucson appears consistently higher (but with at best modest statistical significance) in the rankings of good networks because of its higher performance with respect to the spectral parameters, even though Big Bear had a higher percentage of clear weather. On the other hand, there are several potential advantages of placing a station at Big Bear. Among these are the use of the Tucson prototype instrument as a quasi-independent seventh station for an appreciable fraction of the network operation (estimated at about 30%); and the deployment of the first station at Big Bear as a source of valuable experience in logistics, construction, operation, and data merging under comparatively benign conditions. The final Project decision is to place an instrument at Big Bear, and to maintain Tucson as an alternate.

4.2. Six versus seven sites

One remaining issue is the question of whether the GONG Network should comprise six or seven sites. Analysis shows that the addition of a seventh site (at Urumqi) significantly improves the power spectrum of the window. The improvements are a further reduction (by a factor of three) in the height of the first sidelobe, and increases in the signal-to-noise ratio of the background (SNRB) of 30%, in the first sidelobe (SNFSL) of 63%, and in all side lobes (SNASL) of 37%. The duty cycle of the seven-site network is also slightly higher than the six-site network, rising from 93.95% to 95.07%. The main advantage is gained during the months of July and August, when the Indian monsoon season dominates the conditions at Udaipur. The disadvantages of adding a seventh site at Urumqi are an increase in the cost of the Project, a significant addition to purchases that had already been made, and an increase in the data processing task.

The Project finally decided not to place a seventh instrument of Urumqi, after estimating the impact of the differences between six- and seven-site networks on the scientific goals of the Project. The scientific impact is assessed by examining the effect of the window spectrum sidelobes on the relatively strong p modes and the effects of the window spectrum background on the much weaker g modes.

First, consider contamination of the oscillation spectrum by the fundamental diurnal sidelobe. Since the sidelobe power is proportional to the power of the mode associated with it, the largest effects appear in the region of the p modes where the signal-to-noise ratio is high. An average p mode has an amplitude A of 5 cm s^{-1}, a width, W, of 1 μHz, and power spectral density of $A^2/W = 2500$ (m $s^{-1})^2$ Hz^{-1}. The observed six- and seven-site network window power

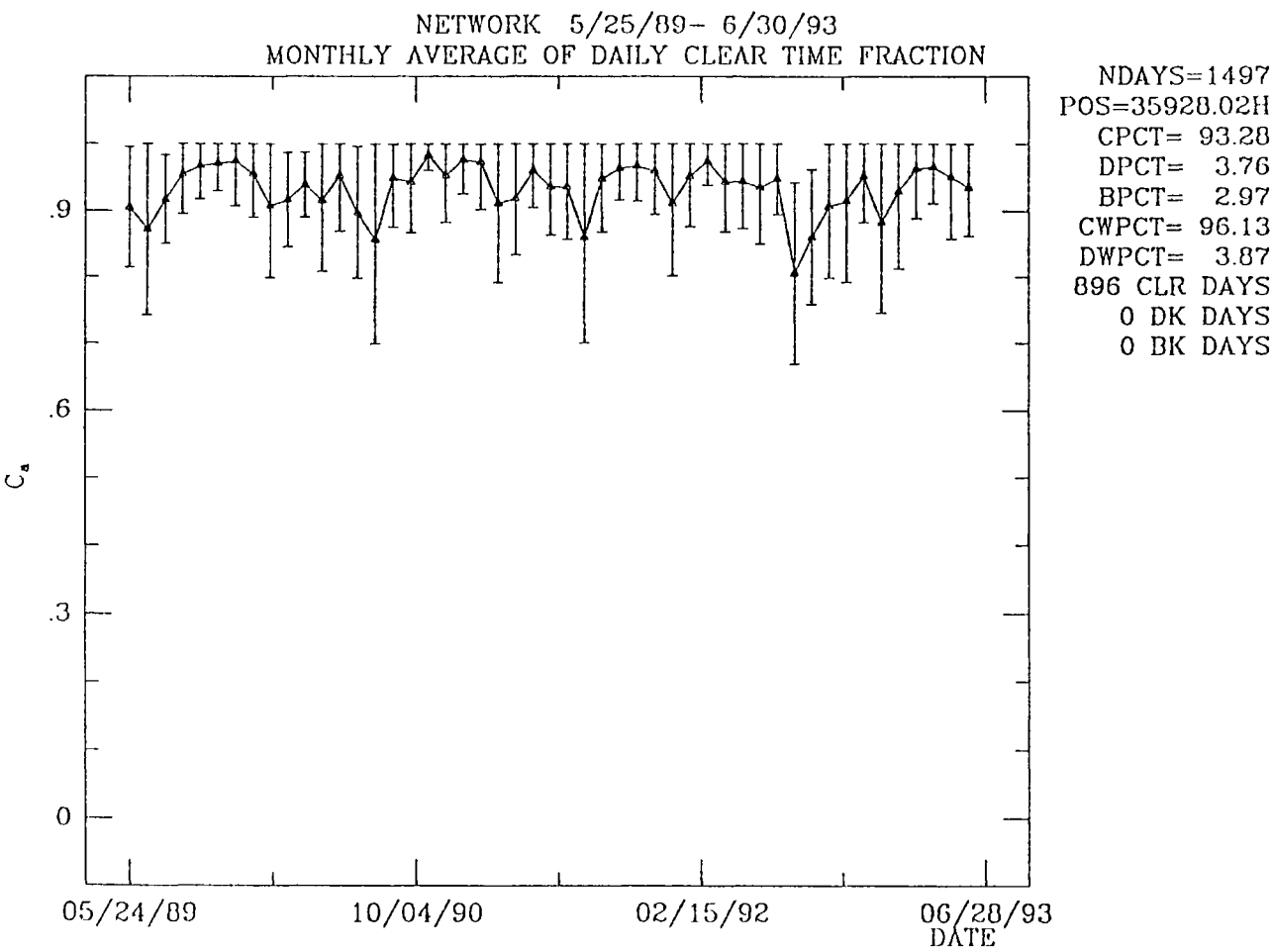

Fig. 7. The monthly average of clear time percentage as a function of time observed with the GONG Network. The vertical bars indicate ± one standard deviation of the monthly data, constrained so that $C_a < 1$.

spectra show that the power of the first sidelobe relative to the main peak is about 4×10^{-4} (six sites), or 1×10^{-4} (seven sites). Thus, an average p mode is surrounded by sidelobes with a height of 1.0 $(\text{m s}^{-1})^2\ \text{Hz}^{-1}$ (six sites), or 0.25 $(\text{m s}^{-1})^2\ \text{Hz}^{-1}$ (seven sites). Measurements of the solar background noise in this region are about 16 $(\text{m s}^{-1})^2\ \text{Hz}^{-1}$ (Jiménez *et al.*, 1988) in agreement with Harvey (1985). Thus the p-mode sidelobes in the six-site window spectrum are already more than an order of magnitude smaller than the solar noise.

Next, consider the overall background of the window spectrum, which affects the detectability of g modes. Again, we compare the estimated effects of the window spectrum and the solar background noise. Since there are no reliable measurements of the properties of g modes, consider a hypothetical g mode with $A = 1\ \text{mm s}^{-1}$, $W = 0.1\ \mu\text{Hz}$, and power spectral density of 10 $(\text{m s}^{-1})^2\ \text{Hz}^{-1}$. The observed background power densities relative to the main paeak are 7×10^{-6} (six sites), or 5×10^{-6} (seven sites). Thus, the background power density from the hypothetical g mode is 7×10^{-5} $(\text{m s}^{-1})^2\ \text{Hz}^{-1}$ (six sites), or 5×10^{-5} $(\text{m s}^{-1})^2\ \text{Hz}^{-1}$ (seven sites). However, since the background is broad-band, we combine the overlapping backgrounds from several g modes. Theory predicts about 20 g modes within

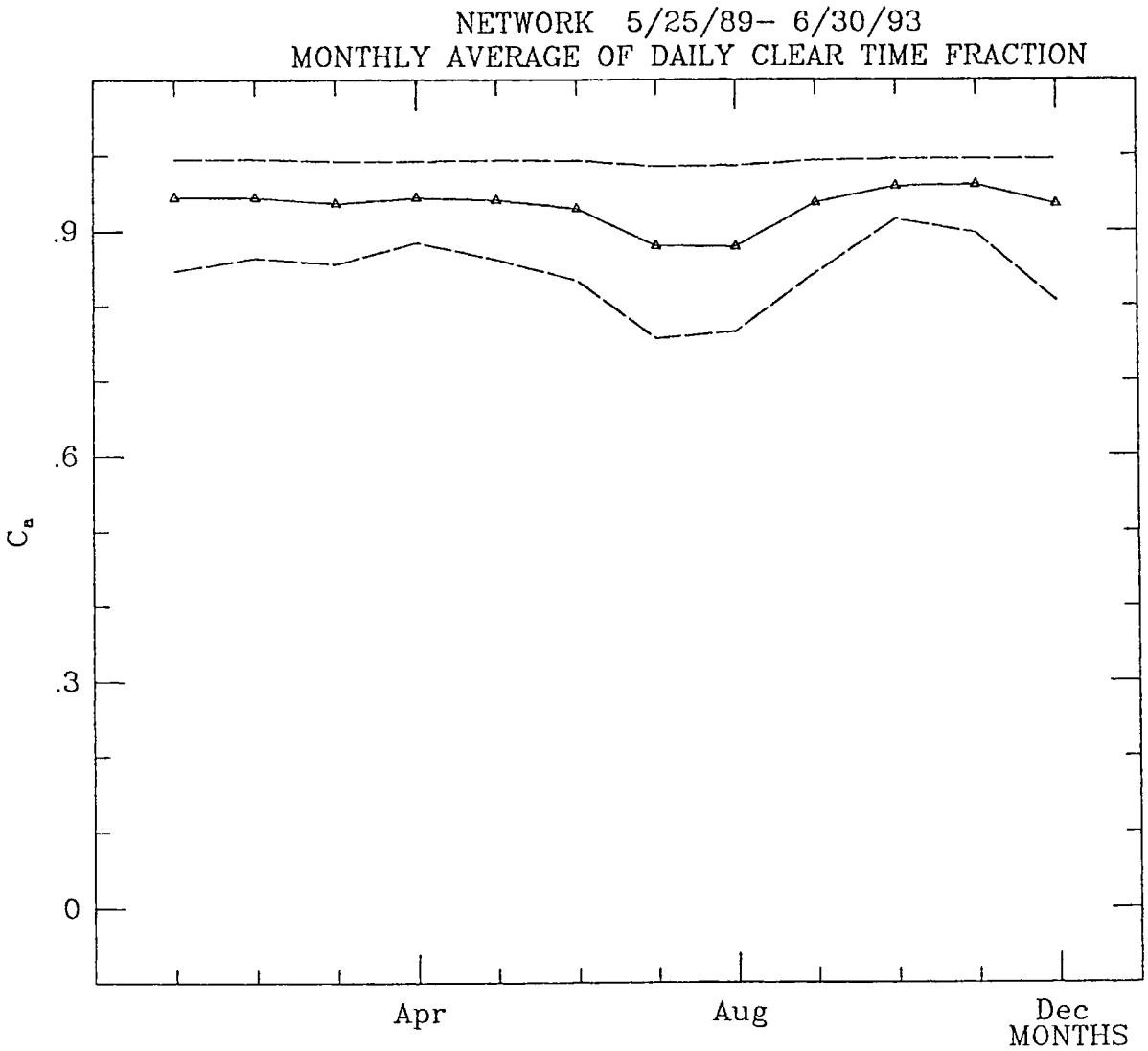

Fig. 8. The calendar month average of the clear time fraction observed by the GONG Network.

60 μHz at a given l in the more crowded regions of the g-mode spectrum. Thus, the total estimated low-frequency background is 1.4×10^{-3} (m s^{-1})^2 Hz^{-1} (six sites), or 1×10^{-3} (m s^{-1})^2 Hz^{-1} (seven sites). The measured average solar background is 1200 (m s^{-1})^2 Hz^{-1} in the 100 to 160 μHz band, so the performance of the six-site network is again completely adequate.

It is also necessary to estimate the amount of noise in the g-mode band from the interaction of the solar background (instead of the g modes) with the network observing window. For a one-month time series there are 156 frequency points in a 60-μHz band, each surrounded by the window spectrum. The total noise added by the window is then roughly 156×1200 (m s^{-1})^2 Hz^{-1} $\times 7 \times 10^{-6} =$ 1.3 (m s^{-1})^2 Hz^{-1} (six sites), or 0.9 (m s^{-1})^2 Hz^{-1} (seven sites). The estimated additional background noise generated by the six-site window is well below the 10 (m s^{-1})^2 Hz^{-1} of the hypothetical g mode.

These results lead to Project to conclude that the addition of a seventh site at

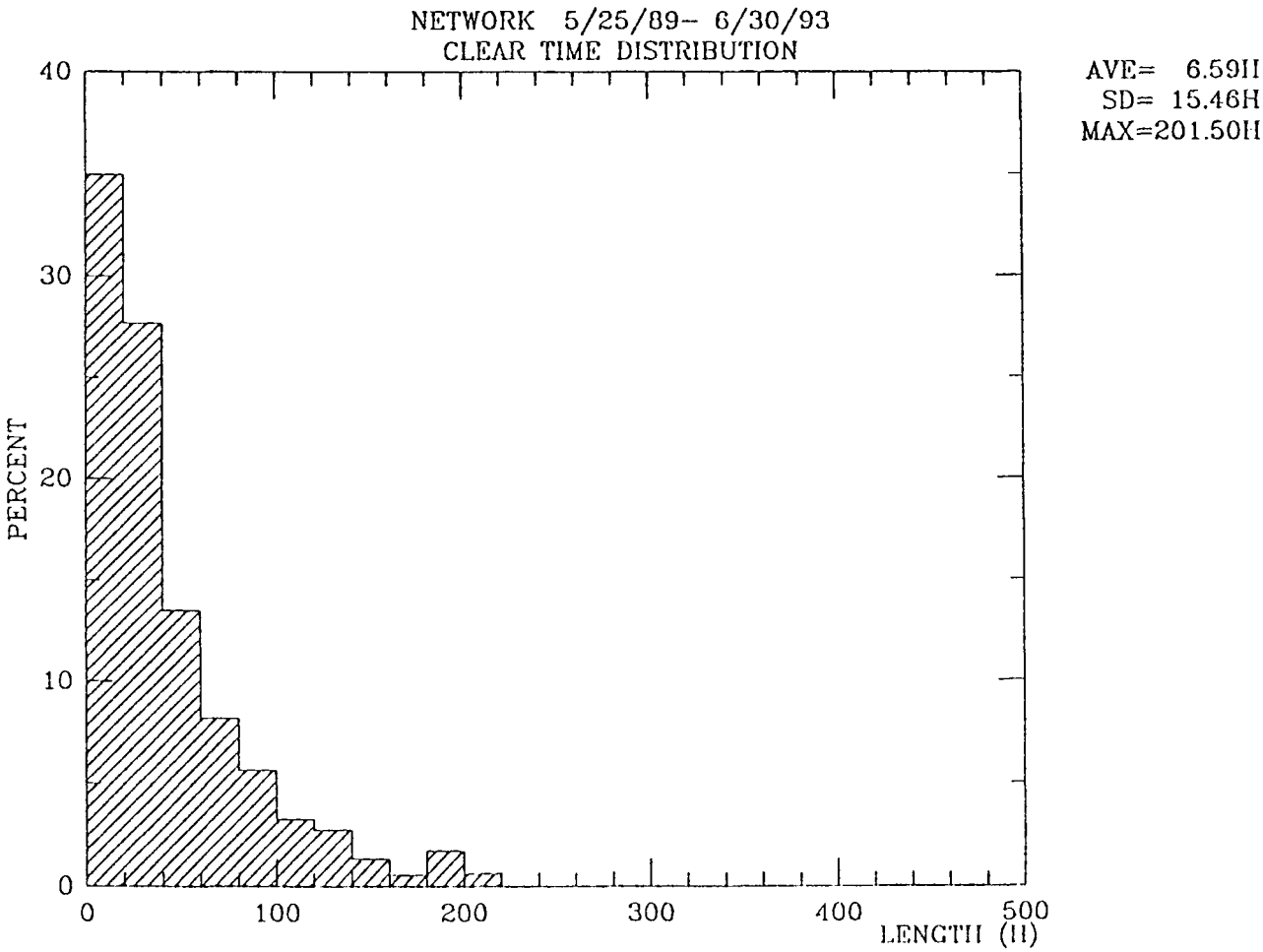

Fig. 9. The distribution of the length of clear time obtained by the GONG Network.

Urumqi is not cost-effective. While the network window is indeed improved, the six-site window is entirely adequate for the project, and the additional expense in funds, labor, and data-reduction effort is not justified. Indeed, spatial leakage due to the limited visible area of the solar surface is likely to be much stronger than any residual temporal leakage in a six-site network window.

4.3. THE GONG NETWORK

The final GONG Network comprises six sites at Big Bear Solar Observatory, California, U.S.A.; the High Altitude Observatory station at Mauna Loa, Hawaii, U.S.A.; Learmonth, Solar Observatory, Australia; Udaipur Solar Observatory, India; the Observatorio de Teide, Tenerife, Canary Islands, Spain; and Cerro Tololo Interamerican Observatory, Chile. A seventh development instrument will be maintained at the Project headquarters in Tucson, Arizona, U.S.A. Note that sites are chosen to optimize the integrated performance of the GONG network for helio-

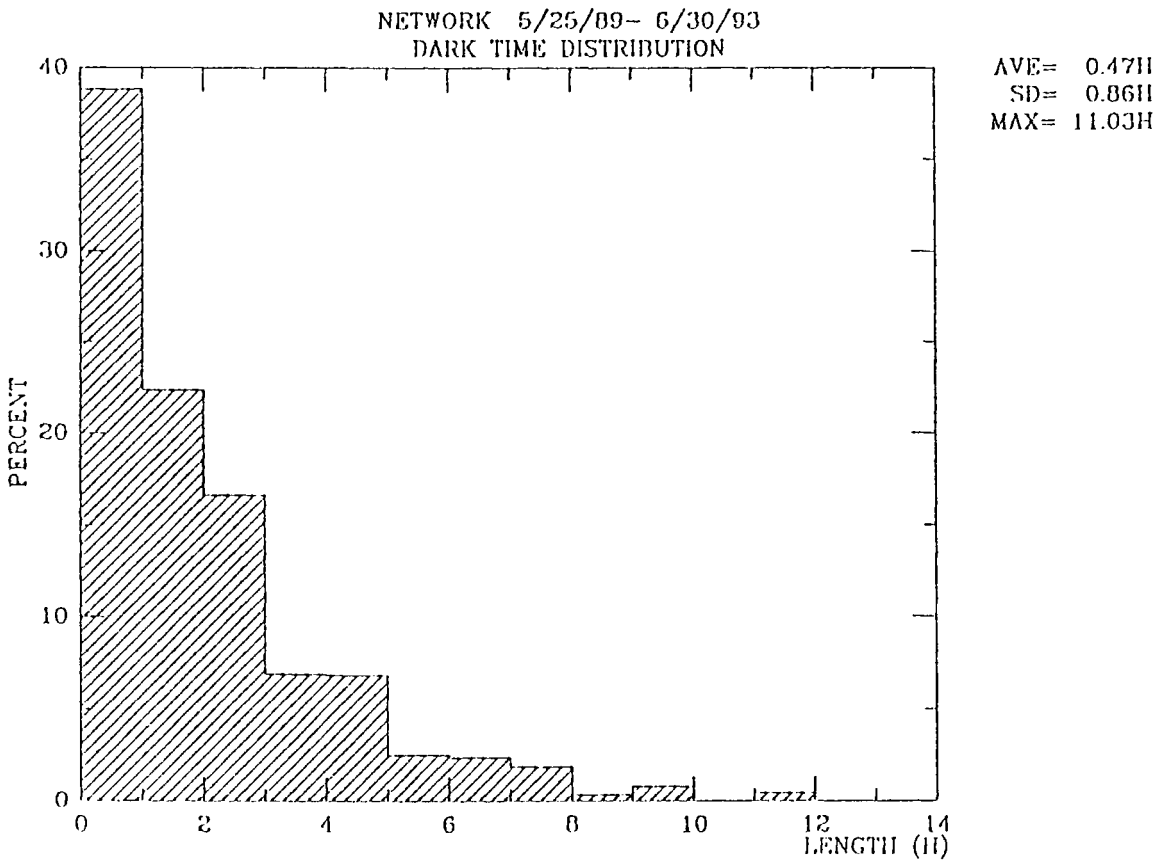

Fig. 10. The distribution of the length of dark time in the GONG Network observing window.

seismology. This should in no way be construed as indicative of the utility of any of the unselected sites for other astronomical purposes.

As of March 1994, data continues to be collected by the site survey instruments at the six selected sites as well as Tucson. Figures 7–11 show the most recently available analysis of the GONG network performance. Figure 7 displays the monthly average of clear time percentage as a function of time. The value ranges from 80.56% to 98.73%, with an averge value of 93.28%. This figure is in excellent agreement with the value of 93.5% predicted by Hill and Newkirk (1985). Figure 8 shows the averge over the more than four-year span of the clear time fraction for each calendar month. The low of 87.98% occurs in August, and the high of 96.10% is in November. Figure 9 provides a histogram of the distribution of the length of clear time obtained by the network. The maximum length of clear time was 201.50 hours, occurring in mid-November of 1989. Figure 10 displays the distribution of the length of dark time. The network was unable to observe the Sun for a maximum length of only 11.03 hours on 5 August, 1990. Figure 11 shows the power spectrum of the window of the network. Comparison of the spectrum with that of a single site for the same time period shows that the fundamental diurnal sidelobe has been reduced by a factor of 1300, and the background noise has been

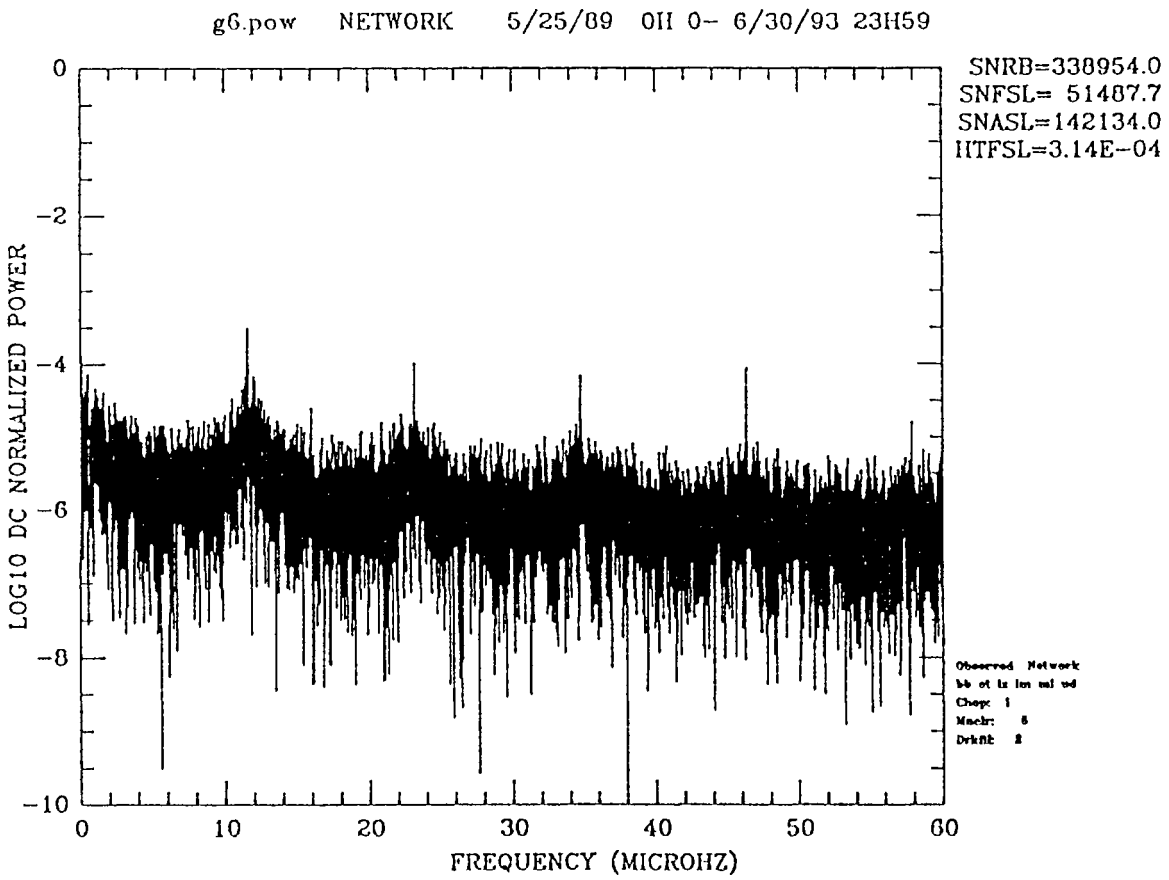

Fig. 11. The power spectrum of the GONG Network window.

reduced by a factor of 50.

4.4. THE EFFECT OF ADDITIONAL INSTRUMENTAL DOWNTIME

The above results are obtained using windows that had been observed with the GONG Site Survey Instrument. However, the Site Survey Instrument is far less complex than the Doppler science instrument. In an effort to predict the future performance of the network with a more complex (and hence possibly less robust) instrument, the observed downtime is increased at each station by factors ranging from 2 to 10. The network window is then constructed and analyzed in the usual manner. The clear time percentage and fundamental diurnal sidelobe height as a function of the increase in downtime are presented in Figures 12 and 13, respectively. This study shows that the six-site network is satisfyingly robust, even in the extreme case of a tenfold increase in time loss. In the worst case, the fraction of observing time is 85.88%, and the height of the first sidelobe in the power spectrum is 0.2%, still far below the sidelobe height in a single-site window. For comparison, the six-site survey instruments over the same period achieve a combined observing time fraction of 93.63%, and a sidelobe height of 0.04%.

To assess the effect of a degraded network on the science, consider the worst case

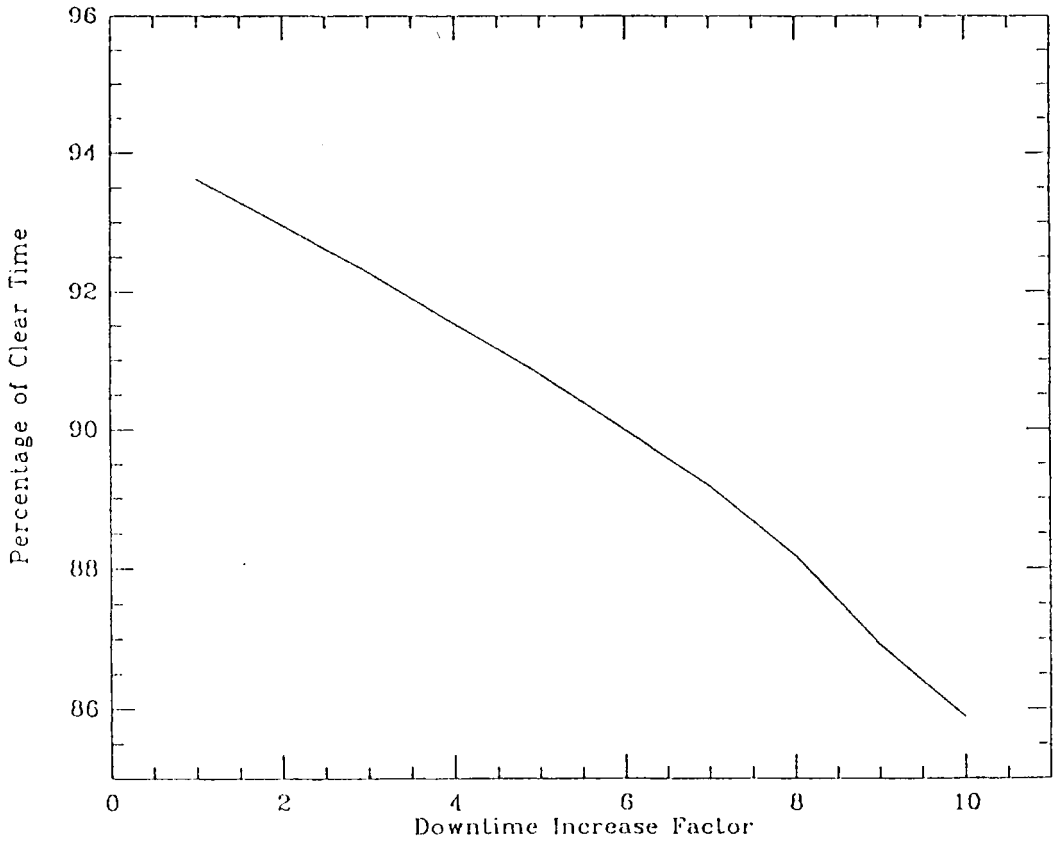

Fig. 12. The clear time fraction of the GONG Network as a function of the increase in downtime. This estimates the performance of a network of instruments more complex than the simple site survey device.

of a tenfold increase in downtime. Then the relative power of the first sidelobe rises to 2×10^{-3}. Performing the same calculation as described in Section 4.2 results in a noise estimate of 6 $(\mathrm{m\ s^{-1}})^2\ \mathrm{Hz^{-1}}$ arising from the sidelobes around the p modes. This number is to be compared again with the 16 $(\mathrm{m\ s^{-1}})^2\ \mathrm{Hz^{-1}}$ level of the solar background. The network performs adequately, even in this scenario. For the g-mode background of 4×10^{-3} $(\mathrm{m\ s^{-1}})^2\ \mathrm{Hz^{-1}}$, still far below the 10 $(\mathrm{m\ s^{-1}})^2\ \mathrm{Hz^{-1}}$ g-mode power density. The estimated additional noise due to the interaction of the solar background and the window function rises to 3.8 $(\mathrm{m\ s^{-1}})^2\ \mathrm{Hz^{-1}}$, still below the 10 $(\mathrm{m\ s^{-1}})^2\ \mathrm{Hz^{-1}}$ of the hypothetical g mode, and well below the 1200 $(\mathrm{m\ s^{-1}})^2\ \mathrm{Hz^{-1}}$ estimated level of the solar background in the g-mode regime. Again, the network is seen to perform adequately.

5. Conclusions

The GONG Site Survey compared the observing conditions necessary for helioseismology at 15 sites around the world. From these, six sites at Big Bear, Mauna Loa, Learmonth, Udaipur, Teide, and Cerro Tololo were selected to comprise the GONG Network. The selection of the sites was based on the integrated perfor-

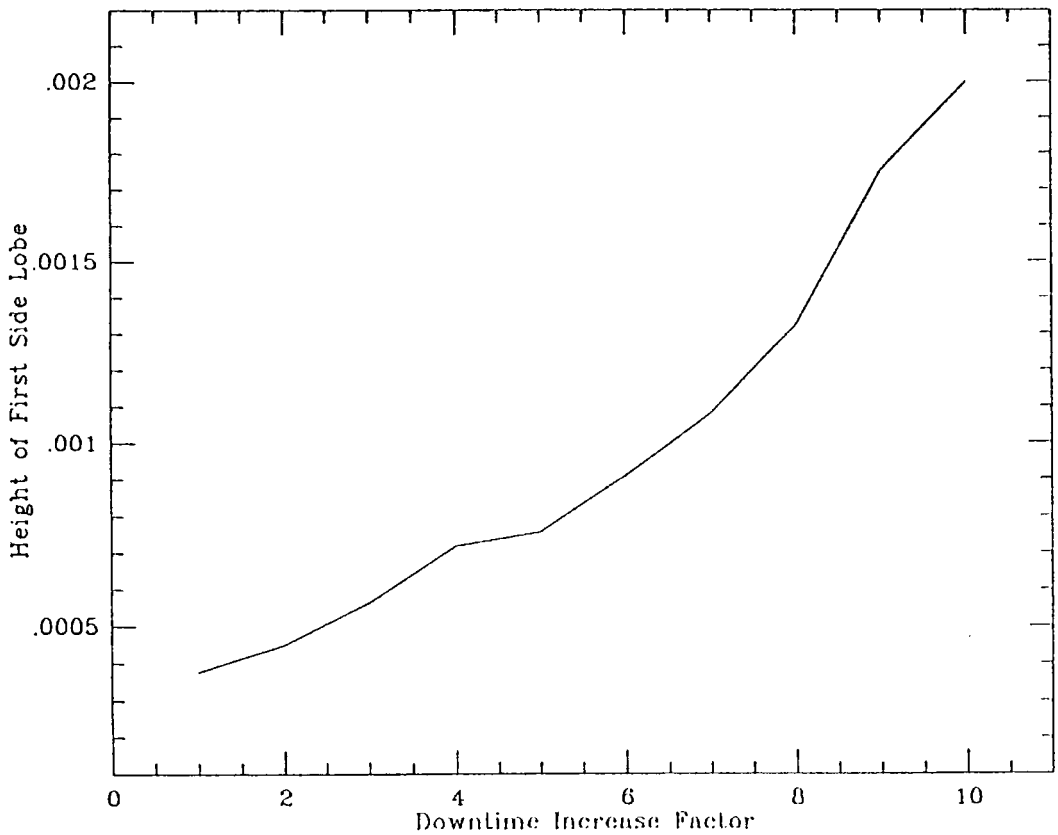

Fig. 13. The height of the first diurnal sidelobe as a function of increasing downtime.

mance of the GONG network, and should in no way be construed as indicative of the utility of any of the unselected sites for other astronomical purposes.

The site survey also results in extensive measurements of the clear weather percentage, extinction coefficient, and transparency power spectrum at the candidate sites. These measurements may be useful to other investigators interested in aspects of the Earth's atmosphere.

Acknowledgements

This work utilizes data obtained by the Global Oscillation Network Group (GONG) project, managed by the National Solar Observatory, a Division of the National Optical Astronomy Observatories, which is operated by AURA, Inc. under a cooperative agreement with the National Science Foundation.

The GONG Project is composed of many people. At last count, approximately 200 people around the world had contributed to the site survey alone. The effort of these dedicated workers is greatly appreciated by the authors and the GONG.

References

Aindow, A., Elsworth, Y. P., Isaak, G. R., McLeod, C. P., New, R., and van der Raay, H. B.: 1988, in E. J. Rolfe (ed.), *Seismology of the Sun and Sun-Like Stars*, ESA SP-286, Paris, p. 157.

Ambastha, A. and Bhatnagar, A.: 1985, *Photographic Atlas of the Solar Chromosphere*, Udaipur Solar Observatory, Udaipur.

Ambastha, A., Bhatnagar, A., Jain, R., Srivastava, N., Gupta, S., Sharma, R., Agrawal, G., Kumawat, V., Hill, F., Fischer, G., Grier, J., Jones, H. P., Jones, P., Kupke, R., Leibacher, J. W., and Stebbins, R. T.: 1991, *Bull. Astron. Soc. India* **19**, 215.

Benkhaldoun, Z., Kadiri, S., Lazrek, M., and Touma, H.: 1991, *Solar Phys.* **133**, 61.

Benkhaldoun, Z., Kadiri, S., Lazrek, M., and Vernin, J.: 1993, *Exper. Astron.* **2**, 345.

Brandt, P. N. and Wöhl, H.: 1982, *Astron. Astrophys.* **109**, 77.

Fischer, G., Hill, F., Jones, W., Leibacher, J., McCurnin, W., Stebbins, R., and Wagner, J.: 1986, *Solar Phys.* **103**, 33.

Fossat, E.: 1991, *Solar Phys.* **133**, 1.

Harvey, J. W.: 1985, in E. J. Rolfe and B. Battrick (eds.), *Future Missions in Solar, Heliospheric, and Space Plasma Physics*, ESA SP-235, p. 199.

Hill, F.: 1990, in G. Berthomieu and M. Cribier (eds.), *Inside the Sun*, Kluwer Academic Publishers, Dordrecht, Holland, p. 265.

Hill, F. and the GONG Site Survey Team: 1988, in E. J. Rolfe (ed.), *Seismology of the Sun and Sun-Like Stars*, ESA SP-286, Paris, p. 209.

Hill, F. and Newkirk, G., Jr.: 1985, *Solar Phys.* **95**, 201.

Hill, F., Fischer, G., Grier, J., Leibacher, J. W., Jones, H. P., Jones, P., Kupke, R., and Stebbins, R. T.: 1994, *Solar Phys.* **152**, 321 (this issue, Paper I).

Jiménez, A., Pallé, P. L., Peréz Hernández, F., Régulo, C., and Roca Cortés, T.: 1988, *Astron. Astrophys.* **192**, L7.

Kennewell, J. A. and Cornelius, D. W.: 1983, *Australian Phycisist* **20**, 276.

Pallé, P. L.: 1991, *Solar Phys.* **133**, 65.

Zirin, H. and Mosher, J. M.: 1988, *Solar Phys.* **115**, 183.